⌘ *Author's Choice*

# *Xenopus laevis* Ctc1-Stn1-Ten1 (xCST) Protein Complex Is Involved in Priming DNA Synthesis on Single-stranded DNA Template in *Xenopus* Egg Extract*[S]

**Hidenori Nakaoka, Atsuya Nishiyama[1], Motoki Saito[2], and Fuyuki Ishikawa[3]**

*From the Laboratory of Cell Cycle Regulation, Department of Gene Mechanisms, Graduate School of Biostudies, Kyoto University, Yoshida-Konoe-cho, Sakyo-ku, Kyoto 606-8501, Japan*

**Background:** The Ctc1-Stn1-Ten1 (CST) complex has been identified as a telomere-associated single-stranded (ss) DNA-binding protein complex.
**Results:** *De novo* priming on ssDNA template in *Xenopus* egg extracts was inefficient in the absence of CST.
**Conclusion:** CST regulates pre-RC (pre-replication complex)-independent DNA replication initiation.
**Significance:** This study contributes to our understanding of the replication mechanism of telomere DNA.

The Ctc1-Stn1-Ten1 (CST) complex is an RPA (replication protein A)-like protein complex that binds to single-stranded (ss) DNA. It localizes at telomeres and is involved in telomere end protection in mammals and plants. It is also known to stimulate DNA polymerase α-primase *in vitro*. However, it is not known how CST accomplishes these functions *in vivo*. Here, we report the identification and characterization of *Xenopus laevis* CST complex (xCST). xCST showed ssDNA binding activity with moderate preference for G (guanine)-rich sequences. xStn1-immunodepleted *Xenopus* egg extracts supported chromosomal DNA replication in *in vitro* reconstituted sperm nuclei, suggesting that xCST is not a general replication factor. However, the immunodepletion or neutralization of xStn1 compromised DNA synthesis on ssDNA template. Because primed ssDNA template was replicated in xStn1-immunodepleted extracts as efficiently as in control ones, we conclude that xCST is involved in the priming step on ssDNA template. These results are consistent with the current model that CST is involved in telomeric C-strand synthesis through the regulation of DNA polymerase α-primase.

ssDNA is physically and chemically less stable than duplex DNA. Thus, it needs to be protected by ssDNA-binding proteins (SSBs)[4] (1, 2). Generated in the intermediate steps of DNA replication, repair, and recombination, ssDNA shows typically transient existence. The ends of linear chromosomes, telomeres, however, naturally possess 3′-overhangs consisting of guanine-rich telomere repeats (G-overhang) in which SSBs are the constitutive structural components. In budding yeast *Saccharomyces cerevisiae*, a trimeric protein complex composed of Cdc13p, scStn1p (suppressor of *cdc13*), and scTen1p (telomeric pathways in association with Stn1, number 1) plays a protective role in telomeres. All the three genes are essential, and a series of temperature-sensitive mutants showed abnormal telomere lengths, long telomeric 3′-overhangs, and activation of the DNA damage checkpoint (3, 4). We and another group have identified Stn1 and Ten1 homologs in mammals and plants, respectively. Furthermore, a new gene product named Ctc1 (conserved telomere maintenance component 1) was found to form an RPA (replication protein A)-like trimeric complex with Stn1 and Ten1 (CST complex). *CTC1* or *STN1* knockdown in mammalian cell lines resulted in G-overhang extension, DNA damage response, and sporadic telomere loss, whereas *ctc1* mutant plants showed severe telomere length deregulation phenotype and growth defects (5, 6). Together, these results demonstrated the presence of a conserved mechanism of telomere end protection from yeast to human (5–8).

RPA is also known to bind to the telomeric 3′-overhang in the S phase and to be involved in the regulation of telomere length (9–12). It is also required for DNA damage checkpoint activation at deprotected telomeres (13).

Another known telomere-associated SSB is POT1 (protection of telomeres 1), which is conserved in a wide range of eukaryotes, including fission yeast, mammals, and plants, and binds with high affinity to G-rich telomeric repeat sequences. It is believed that POT1 precludes RPA from binding to the G-overhangs and activating the DNA damage signaling pathways (14). Interestingly, POT1 does not seem to compete with CST in binding to telomeres, and the two are redundantly required to prevent chromosomal ends from being recognized as DNA damage (5).

⌘ *Author's Choice*—Final version full access.
[S] This article contains supplemental Figs. S1–S8.
[1] Present address: Institute of Human Genetics, CNRS, 34396 Montpellier, France.
[2] Present address: Pharmaceutical and Healthcare Research Laboratories, Fujifilm Corp., 577 Ushijima, Kaisei-machi, Ashigarakami-gun, Kanagawa 258-8577, Japan.
[3] To whom correspondence should be addressed. Tel.: 81-75-753-4196; Fax: 81-75-753-4197; E-mail: fishikaw@lif.kyoto-u.ac.jp.
[4] The abbreviations used are: SSB, single-stranded DNA-binding protein; CST, Ctc1-Stn1-Ten1; Ctc1, conserved telomere maintenance component 1; ds, double stranded; ELB, egg lysis buffer; HSS, high speed supernatant; LSS, low speed supernatant; NPE, nucleoplasmic *Xenopus* egg extract; NTA, nitrilotriacetic acid; OB-fold, oligosaccharide/oligonucleotide binding fold;

POT1, protection of telomeres 1; RPA, replication protein A; xCST, *Xenopus* CST.

Taken together, at least three kinds of SSBs can bind to chromosomal ends depending on the situation. Although the simplest view is that CST and POT1 protect telomeres by antagonistically excluding RPA from telomeres, some DNA damage responses may be required to form the appropriate telomere structures during and/or after telomere replication (15). Thus, it is necessary to know how the different SSBs are coordinately targeted and function at a defined site to understand not only telomere biology but also other biological processes involving multiple SSBs.

It has been reported that scStn1 interacts physically and genetically with the regulatory subunit of DNA polymerase $\alpha$, raising the possibility that Stn1 regulates the lagging DNA synthesis at telomeres (8, 16). In parallel with our identification of mammalian CST, another group reported that AAF-132 and AAF-44, which had been identified as mouse DNA polymerase $\alpha$-primase accessory proteins, regulate DNA replication in mammalian cells (17). Because AAF-132 and AAF-44 were found to be identical to Ctc1 and Stn1, respectively, it is important to clarify whether or not mammalian CST plays a role in the telomeric C-strand replication by DNA polymerase $\alpha$-primase. Although AAFs are suggested to be general DNA replication factors, our recent study challenged this idea by showing that endogenous human STN1 (hStn1) did not co-localize with DNA replication foci (5). It is still open to debate, however, when and where CST (AAFs) functions in cells.

To investigate these issues further, we utilized *Xenopus* egg extracts because they serve as excellent *in vitro* DNA replication model systems (18). *Xenopus* egg extracts are cell-free systems that can be easily manipulated by immunodepleting the proteins of interest or adding various types of reagents. Unlike *in vitro* systems that are reconstituted with purified proteins and defined chemicals, *Xenopus* egg extracts include essentially all factors that support early embryonic development and therefore faithfully recapitulate cellular events, including cell cycle progression. We describe herein the identification of *Xenopus laevis* CST and its involvement in priming DNA synthesis on ssDNA template in the egg extracts. Our data also showed that xCST is not an absolute requirement for chromosomal DNA replication. Our results are consistent with the hypothesis that CST is involved in the lagging strand synthesis in concert with DNA polymerase $\alpha$-primase at telomeres, in addition to its protective function.

## EXPERIMENTAL PROCEDURES

### Identification and Cloning of Xenopus laevis Ctc1, Stn1, and Ten1

The *X. laevis* expressed sequence tag data base, Xenbase, was searched for *Xenopus* transcripts potentially encoding Ctc1, Stn1, and Ten1, using the amino acid sequences of human homologs as queries. Full-length cDNAs were obtained by conventional RT-PCR techniques using total RNA derived from unfertilized *Xenopus* eggs. The alignments of the *Xenopus* and human amino acid sequences were performed using the ClustalW program on the website of DNA Data Bank of Japan.

### Antibodies and Recombinant Proteins

We immunized two rabbits with full-length xStn1 recombinant protein (N-terminally His$_{10}$-tagged, expressed in *Escherichia coli* BL21-Codonplus (DE3) and purified using Ni-NTA-agarose (Qiagen)) to raise anti-xStn1 antibodies and obtained two lots of antisera, KU003 and KU004. IgG was affinity-purified using the antigen-blotted membrane. KU004 was used in all experiments except the one shown in Fig. 6. Anti-polymerase $\alpha$ p180 (DNA polymerase $\alpha$ catalytic subunit) antiserum, anti-mouse Prim1 (primase p49 subunit) antiserum, anti-H3 rat monoclonal antibody, and anti-*Xenopus* RPA p34 mouse monoclonal antibody were kindly provided by Dr. S. Waga (Japan Women's University), Dr. T. Mizuno (RIKEN), Dr. H. Kimura (Osaka University), and Dr. M. Méchali (Institute of Human Genetics, CNRS), respectively. Anti-Mcm7 mouse monoclonal antibody was purchased from Abcam (abcam 2360-500). Anti-xRpa1 rabbit polyclonal antibody was generated against full-length recombinant protein.

To prepare recombinant xCST, Sf9 insect cells were infected simultaneously with baculoviruses expressing 3×FLAG-xCtc1, His$_6$-xStn1, and His$_6$-xTen1. Approximately $1 \times 10^8$ infected cells were harvested and lysed with 60 ml of buffer A (10 mM PIPES-NaOH, pH 6.8, 300 mM sucrose, 500 mM NaCl, 3 mM MgCl$_2$, and 0.2% Triton X-100) supplemented with Complete EDTA-free (Roche Applied Science). Then, the lysate was clarified by ultracentrifugation using a TLA-110 rotor (Beckman) at $120,000 \times g$ (55,000 rpm) for 20 min. The lysate was mixed with 1 ml of anti-FLAG M2 gel (Sigma) overnight. After extensively washing the gel, the bound proteins were eluted with 10 ml of buffer A supplemented with 0.1 mg/ml 3× FLAG peptide (Sigma) and 10 mM imidazole. The eluate was mixed with 0.5 ml of Ni-NTA-agarose for 1 h. After washing the agarose in buffer A containing 50 mM imidazole, the bound proteins were eluted with 3 ml of 500 mM imidazole in buffer A, concentrated to ~50 $\mu$l using a Vivaspin 500 ultrafiltration unit (Sartorius Stedim), and then subjected to gel filtration using Superose 6 PC 3.2/30 (GE Healthcare) column conditioned in buffer A containing 0.1% instead of 0.2% Triton X-100. Twenty-eight fractions measuring 80 $\mu$l each were collected, and 10 $\mu$l was subjected to 13% SDS-PAGE followed by Coomassie Brilliant Blue staining. Fractions 11 and 12, where the majority of the recombinant proteins were found (see Fig. 1C), were mixed, and the aliquots were frozen in liquid nitrogen and stored at −80 °C. xCST(n) was prepared with similar procedures using Talon Metal Affinity Resin (BD Biosciences) and Superose 6 10/300 GL instead of Ni-NTA-agarose and Superose 6 PC 3.2/30.

To prepare recombinant xRPA, cDNAs of xRpa1, xRpa2, and xRpa3 were cloned from total RNA prepared from unfertilized *Xenopus* eggs by RT-PCR, and a simultaneous expression vector in which the three genes were placed in tandem under the regulation of a single T7 promoter was generated using pET19 vector (Novagen) (xRpa1 was tagged with His$_{10}$ at its N terminus whereas the other two had no tags). Bacterial cell pellets from a 1-liter culture of BL21-CodonPlus (DE3) expressing xRPA were suspended in 75 ml of buffer containing 50 mM sodium phosphate, pH 8.0, 500 mM NaCl, 20 mM imidazole, and 1 mg/ml lysozyme and incubated for 15 min on ice. Then, Non-

idet P-40 was added to a final concentration of 0.2%. The lysate was incubated further on ice for 10 min and frozen in liquid nitrogen. The lysate was thawed and cleared by centrifugation with a JA-20 rotor (Beckman) at $18,000 \times g$ (15,000 rpm) for 20 min. Then, 0.5 ml of Ni-NTA-agarose was added, and mixing was carried out for 1 h. After washing the gel, the bound proteins were eluted with 0.5 ml $\times$ 3 of buffer A with a stepwise gradient of imidazole (50, 100, 200, and 500 mM). Fractions containing xRPA were collected, concentrated, and further purified by gel filtration as described above.

To determine the concentrations of xCST and xRPA recombinant preparations, samples were separated by SDS-PAGE and stained with SYPRO Ruby (Molecular Probes). Protein bands were visualized and quantified using a Typhoon 9400 image analyzer (GE Healthcare) and the equipped software, Image Quant.

### Xenopus Egg Extracts

Interphase low speed supernatant (LSS; cytoplasmic *Xenopus* egg extract), high speed supernatant (HSS; cytosolic *Xenopus* egg extract), and nucleoplasmic *Xenopus* egg extract (NPE) were prepared as described (19).

### Chromatin Isolation

*Xenopus* sperm nuclei (3,000 nuclei/$\mu$l) were incubated in 50 $\mu$l of interphase LSS supplemented with 2 mM ATP, 20 mM phosphocreatine, 50 $\mu$g/ml creatine phosphokinase (ATP regeneration system), and 3 $\mu$g/ml nocodazole at 23 °C for the indicated times. The reaction mixture was diluted 10 times with ice-cold egg lysis buffer (ELB) (10 mM HEPES-KOH, pH 7.7, 50 mM KCl, 2.5 mM MgCl$_2$, and 250 mM sucrose) and layered onto 1 ml of sucrose cushion (ELB containing 500 mM sucrose instead of 250 mM). Then, it was centrifuged at $6,100 \times g$ for 10 min at 4 °C. The nuclei pellet was washed once with 1 ml of ELB and resuspended in 1 ml of chromatin isolation buffer (50 mM HEPES-NaOH, pH 7.5, 150 mM KCl, 5 mM MgCl$_2$, 250 mM sucrose, and 0.6% Triton X-100). After a 5-min incubation on ice, the suspended chromatin was precipitated by centrifugation ($6,100 \times g$, 5 min at 4 °C) and washed once with 1 ml of chromatin isolation buffer. The supernatant was completely removed by aspiration using a GELoader Tip (Eppendorf), and the chromatin pellet was dissolved in 80 $\mu$l of SDS-PAGE sample buffer. Depending on the proteins analyzed, 5–20 $\mu$l of the samples was used for immunoblotting.

### Immunodepletion

To immunodeplete xStn1 from 30 $\mu$l of HSS and 20 $\mu$l of NPE, 0.2 volume of rProtein A-Sepharose Fast Flow (GE Healthcare) coupled with 1 $\mu$g of anti-xStn1 IgG was added, and the whole was mixed for 30 min using a rotator at 4 °C. Then, the antibody beads were removed with a hand-made spin column. The procedure was repeated three times (a total of 3 $\mu$g of IgG was used). In all experiments, equal amounts of normal rabbit IgG (Santa Cruz Biotechnology) were used as control (mock immunodepletion).

### Electrophoretic Mobility Shift Assay (EMSA)

Thirty-two-mer oligo-DNA probes were purified by PAGE and labeled with $^{32}$P using T4 polynucleotide kinase (TaKaRa).

Ten $\mu$l of reaction mixture containing 10 mM Tris-HCl, pH 8.0, 50 mM NaCl, 1 mM DTT, 5% glycerol, 1 mM EDTA, 0.02 pmol of labeled DNA probe, and 0.01 pmol of recombinant xCST or xRPA was incubated for 30 min at 23 °C and then subjected to 6% PAGE in 0.1$\times$ TBE (10 mM Tris-HCl, pH 8.4, 9 mM boric acid, and 0.1 mM EDTA) at 4 °C. The gel was dried and exposed to a storage Phosphor screen (Fujifilm). Radioactivity was visualized with a Typhoon 9400 image analyzer.

### Indirect Immunofluorescence and Telomere Fluorescence in Situ Hybridization (FISH)

*Xenopus* sperm nuclei (2,000 nuclei/$\mu$l) were incubated in 50 $\mu$l of interphase LSS supplemented with the ATP regeneration system and 3 $\mu$g/ml nocodazole for 40 min at 23 °C. The reaction was diluted 10 times with ice-cold ELB supplemented with 0.5% Nonidet P-40 and incubated on ice for 5 min. The nuclei were spun onto a poly-L-lysine-coated coverslip through 2 ml of 30% sucrose in ELB, using a TS-7 rotor (Tommy) at $1,500 \times g$ for 8 min. The coverslip was fixed with methanol at $-20$ °C for 10 min, followed by acetone at $-20$ °C for 1 min. Blocking was performed with 0.1% each of skim milk and BSA in PBS supplemented with 50 $\mu$g/ml RNase A for 1 h at room temperature. Incubation with the primary antibody (anti-xStn1 KU004) and the secondary antibody (Alexa Fluor 488 donkey anti-rabbit IgG; Molecular Probes) was carried out in Can Get Signal Immunostain Solution A (Toyobo) (overnight at 4 °C for the primary antibody, 2 h at room temperature for the secondary antibody). After fixation in 4% formaldehyde in PBS, the Cy-3-conjugated peptide nucleic acid probe (CCCTAA)$_3$ was hybridized as described previously (20). Vectashield with DAPI (Vector Laboratories) was used as the mounting medium. Fluorescent images were obtained with a DeltaVision microscope (Applied Precision) equipped with a charged-coupled device camera (Photometrics). Image processing was done with SoftWoRx (Applied Precision) and Photoshop (Adobe) software.

### Replication Assays

*Replication of pBluescript*—Fifteen $\mu$l of xStn1-immunodepleted or mock-immunodepleted HSS supplemented with 40 $\mu$M [$\alpha$-$^{32}$P]dCTP (10 mCi/ml) was mixed with 0.6 $\mu$l of 1 mg/ml pBluescript, and incubation was carried out for 30 min at 23 °C (replication assays were performed at 23 °C throughout this study). Five $\mu$l was withdrawn and mixed with 10 $\mu$l of pre-warmed xStn1-immunodepleted or mock-immunodepleted NPE supplemented with the ATP regeneration system and 10 mM DTT. Three-$\mu$l aliquots were removed at 15, 30, 45, and 60 min, and the reactions were terminated with 100 $\mu$l of Stop solution (1% SDS, 20 mM EDTA, and 0.25 mg/ml glycogen). Then, proteinase K was added to a final concentration of 0.6 mg/ml, and samples were incubated for 1 h at 37 °C. DNA was isolated by phenol-chloroform extraction and ethanol precipitation and analyzed on a 0.8% agarose gel in 0.5$\times$ TBE. The autoradiography procedure is described above.

*Replication of M13*—Ten $\mu$l of xStn1-immunodepleted or mock-immunodepleted HSS and NPE was supplemented with 80 $\mu$M [$\alpha$-$^{32}$P]dCTP (10 mCi/ml) and mixed with 0.5 $\mu$l of 0.2 mg/ml M13 mp18 ssDNA (Virion DNA) (TaKaRa). Three-$\mu$l

aliquots were removed at 30, 60, and 90 min and analyzed as in the case of pBluescript. Quantification of the radioactivity was performed with Image Quant.

To generate primed M13, a 10-$\mu$l reaction mixture containing 0.84 pmol of M13, 1 pmol of 30-mer oligo-DNA 5′-ccggg-taccgagctcgaattcgtaatcatg-3′, and 100 mM NaCl was heated for 3 min at 94 °C using a thermal cycler GeneAmp PCR System 9700 (Applied Biosystems), then slowly cooled down to room temperature. The same annealing procedure was also carried out without the oligo-DNA as control (referred to as nonprimed M13).

Replication efficiency was calculated as described previously (21). Endogenous dNTP concentration was assumed to be 60 $\mu$M each.

### M13 Chromatin Purification through Gel Filtration

Three hundred ng of M13 mp18 DNA was incubated in 30 $\mu$l of xStn1-immunodepleted or mock-immunodepleted HSS supplemented with the ATP regeneration system, 10 $\mu$g/ml nocodazole, and 0.2 mM aphidicolin for 1 h. The mixture was loaded onto a manually packed gel filtration column equilibrated with ELB containing 0.2% Triton X-100, and Sepharose CL-4B (GE Healthcare) was packed in an Econo-Column (Bio-Rad; catalog no. 7370522). The height of the packed resin was ~17 cm, and the bed volume was 3 ml. Elution was carried out with ELB containing 0.2% Triton X-100, and 100-$\mu$l fractions were collected. Ten $\mu$l of each fraction was treated with RNase followed by proteinase K, and DNAs were isolated by phenol-chloroform extraction and ethanol precipitation. DNA was separated on a 0.8% agarose gel with 0.5× TBE and stained with SYBR Gold (Invitrogen). Visualization of the bands was accomplished with Typhoon 9400. Eight $\mu$l of each fraction was used for the immunoblotting experiments.

## RESULTS

*Identification of Xenopus Ctc1, Stn1, and Ten1 Genes—X. laevis* Ctc1, Stn1, and Ten1 genes that encode 1,160, 367, and 120 amino acids, respectively, were identified based on sequence similarities to the corresponding human homologs (GenBank accession numbers AB609592, AB609593, and AB609594, respectively). Similarities and identities among the amino acid sequences of the human and *Xenopus* homologs as deduced by the ClustalW program are shown in Fig. 1A. The secondary structure-based fold recognition programs in BioInfoBank MetaServer predicted the presence of oligosaccharide/oligonucleotide binding folds (OB-folds), a characteristic secondary structure found in all known SSBs (1, 22). The predicted OB-fold-containing regions of xCtc1, xStn1, and xTen1 are shown in Fig. 1A (see also supplemental Fig. S1).

*xCtc1, xStn1, and xTen1 Form a Complex (xCST Complex)—* xCtc1, xStn1, and xTen1 cDNAs were obtained by RT-PCR using total RNA derived from unfertilized *Xenopus* eggs as template and expressed as N-terminally tagged recombinant proteins (3×FLAG-xCtc1, His$_6$-xStn1, and His$_6$-xTen1) using the baculovirus expression system. Protein lysates were obtained from insect cells simultaneously infected with baculoviruses expressing the three proteins individually, and recombinant proteins were purified by sequential affinity purifications using
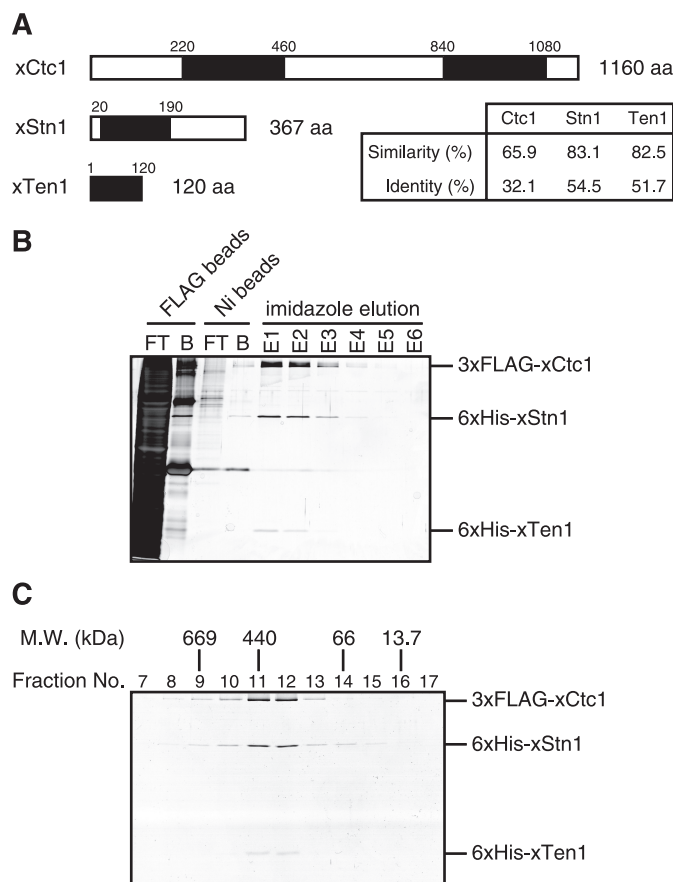


FIGURE 1. **xCtc1, xStn1, and xTen1 form a trimeric complex.** *A.* predicted structures of xCtc1, xStn1, and xTen1 gene products. *Black boxes* represent putative OB-fold-containing regions. Percentages of identical and similar amino acids shared by *Xenopus* proteins and human ones are summarized in the *table. B*, recombinant xCST (3×FLAG-xCtc1, His$_6$-xStn1, and His$_6$-xTen1) expressed in insect cells was affinity-purified using anti-FLAG beads and Ni beads. Proteins were visualized by silver staining. *FT*, flow-through fraction; *B*, bead-bound proteins after elution; *E1* and *E2*, eluate with 100 mM imidazole; *E3* and *E4*, eluate with 200 mM imidazole; and *E5* and *E6*, eluate with 500 mM imidazole. *C*, E1 and E2 fractions in *B* were combined and subjected to gel filtration. Proteins in each fraction were separated by SDS-PAGE, and the gel was stained with Coomassie Brilliant Blue.

anti-FLAG-agarose beads and Ni-agarose beads (Fig. 1B). In an SDS-PAGE analysis, the purified protein fraction contained three major protein bands showing gel mobility compatible with the predicted molecular masses of the recombinant proteins. Then, the affinity-purified proteins were subjected to gel filtration, and xCtc1, xStn1, and xTen1 were eluted in the same fractions, suggesting that the three proteins formed a complex (Fig. 1C).

*xCST Binds to ssDNA with Moderate Preference for G-rich Sequences and Localizes at Telomeres in in Vitro Reconstituted Xenopus Sperm Nuclei—* Mammalian CST has been shown to bind to ssDNA with no apparent sequence preferences (5). To examine whether xCST has similar biochemical activities or not, we performed EMSA using the recombinant proteins shown in Fig. 2A. xRPA, a well characterized SSB (23), was used for comparison. We tested telomeric sequence probes (note that the telomere repeat sequence is conserved in vertebrates, including *Xenopus* species)[5] (24) because the localization of
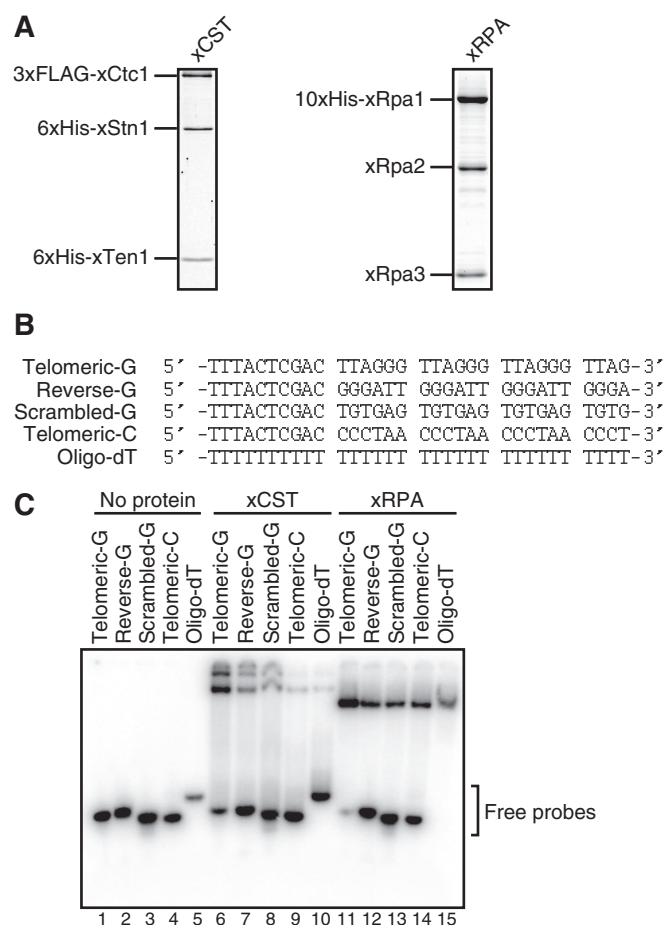
---

[5] K. Muraki and F. Ishikawa, unpublished data.

## A



## B

| | | |
|---|---|---|
| Telomeric-G | 5′ | -TTTACTCGAC TTAGGG TTAGGG TTAGGG TTAG-3′ |
| Reverse-G | 5′ | -TTTACTCGAC GGGATT GGGATT GGGATT GGGA-3′ |
| Scrambled-G | 5′ | -TTTACTCGAC TGTGAG TGTGAG TGTGAG TGTG-3′ |
| Telomeric-C | 5′ | -TTTACTCGAC CCCTAA CCCTAA CCCTAA CCCT-3′ |
| Oligo-dT | 5′ | -TTTTTTTTTT TTTTTT TTTTTT TTTTTT TTTT-3′ |

## C



FIGURE 2. **xCST binds to ssDNA with moderate preference for G-rich sequences.** *A*, preparation of recombinant xCST and xRPA used in EMSA. Proteins were visualized by SYPRO Ruby staining of SDS-polyacrylamide gel. *B*, sequences of 32-mer ssDNA probes used in EMSA. *C*, EMSA. The reaction mixtures included 20 nM $^{32}$P-labeled DNA probes and 10 nM xCST (*lanes 6–10*) or 10 nM xRPA (*lanes 11–15*). For *lanes 1–5*, control buffer was included instead of protein samples.

## A



## B



FIGURE 3. **xStn1 associates with chromatin and localizes at telomeres.** *A*, xStn1 localization in *in vitro* reconstituted *Xenopus* sperm chromatin was analyzed by indirect immunofluorescence in combination with telomere FISH. A representative set of microscopic images is shown. DNA stained with DAPI is shown in *blue*. *White arrowheads* indicate the co-localization of xStn1 foci (*green*) and telomeric FISH signals (*red*). Enlarged images of the *numbered white boxes* on the merged picture are shown on the *right*. *B*, *Xenopus* sperm nuclei were incubated in interphase LSS for the indicated times. The time when sperm nuclei were added to the egg extract was set to 0 min. Isolated chromatin was analyzed by immunoblotting using the indicated antibodies. The reaction mixtures contained control buffer (*lanes 1–4*), 60 μg/ml GST-geminin H (*lanes 5–8*), or 50 μg/ml aphidicolin (*lanes 9–12*), respectively.

CST at telomeres had been argued in previous work (Fig. 2*B*). Unlike mammalian CST, xCST moderately preferred the G-rich probes to the telomeric-C and oligo(dT) probes (Fig. 2*C*, compare *lanes 6–8* with *lanes 9* and *10*). This was further confirmed by a competition experiment (supplemental Fig. S2). These results contrast with those of xRPA; xRPA bound to all the probes with the highest affinity being toward the oligo(dT) probe (Fig. 2*C*, *lanes 11–15*). Indirect immunofluorescence staining revealed discrete foci of xStn1 in *in vitro* reconstituted *Xenopus* sperm nuclei, demonstrating the association of xStn1 with chromatin. We also found that a fraction of those foci co-localized with telomere FISH signals (Fig. 3*A*), in agreement with the observed G-preference of xCST. xStn1 foci were observed in most nuclei (18 of 20).

*xStn1 Binds to Chromatin Independently of Chromosomal Replication*—When incubated in interphase LSS, *Xenopus* sperm nuclei are replicated; extensive DNA synthesis occurs from 0.5 to 1 h after the addition of the nuclei, and the reaction completes within 2 h. xStn1 binding to chromatin during the time course of replication was analyzed to determine whether it is correlated with DNA replication. Whereas the association of the replication-related proteins (Polα, Mcm, and RPA) peaked
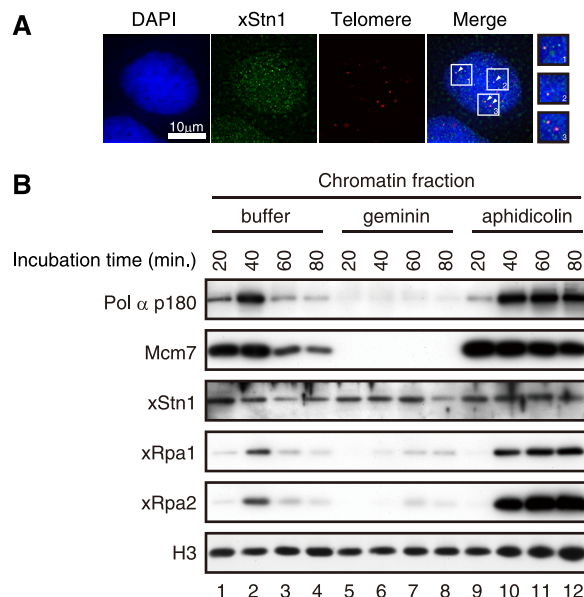
at around 40 min and was barely detectable when pre-RC formation was blocked by geminin (a licensing inhibitor), xStn1 almost constantly bound to chromatin during the time course, and its association was replication-independent (Fig. 3*B*, *lanes 1–8*). Furthermore, xStn1 did not accumulate on aphidicolin-treated chromatin, on which replication-related proteins eminently accumulated due to replication fork stalling and extensive ssDNA exposure (Fig. 3*B*, *lanes 9–12*) (25, 26). These results suggest that xStn1 (xCST) has a role other than chromosomal replication.

*xCST Is Not Required for Bulk Chromosomal Replication but Is Involved in Replication on ssDNA Template*—Circular plasmids undergo a single round of pre-RC-dependent semiconservative replication when incubated consecutively in HSS and NPE (19). To test directly whether xStn1 is involved in the semiconservative replication or not, we prepared xStn1-immunodepleted or mock-immunodepleted HSS and NPE (Fig. 4*A*) and assayed for DNA replication using circular pBluescript plasmid double-stranded (ds)DNAs as the template. Neither the amount of replicated DNA nor the replication kinetics was affected in any combination of extracts (Fig. 4*B*, *upper*). For detailed explanations of each band appearing on pBluescript and below described M13 replication assays, see supplemental Fig. S4). The chromosomal replication of *in vitro* reconstituted *Xenopus* sperm nuclei in LSS took place in xStn1-immunodepleted LSS as efficiently as in mock-immunodepleted LSS (supplemental Fig. S5). These results demonstrate that xStn1 (presumably xCST) is dispensable for the pre-RC-dependent replication of duplex DNA.
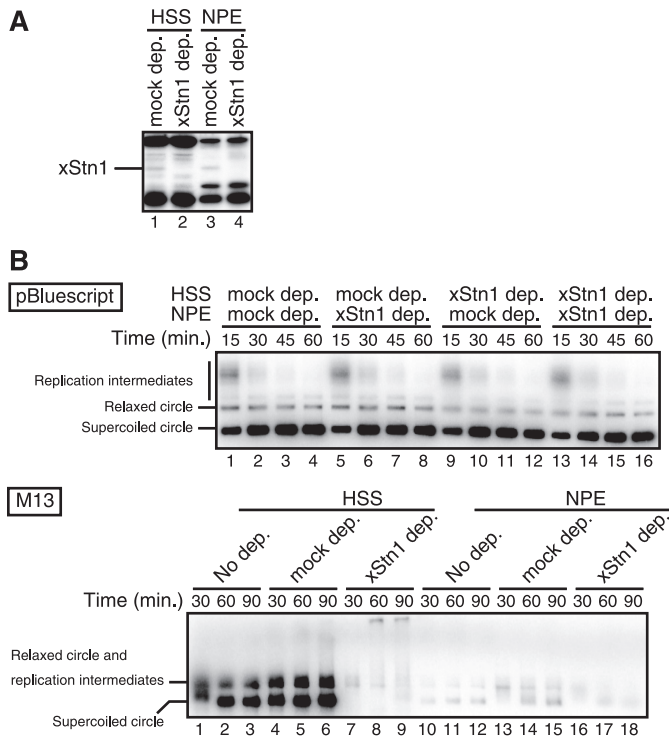
**A**



**B**



FIGURE 4. **xStn1 is required for priming on ssDNA template but not essential for bulk chromosomal replication.** *A*, xStn1-immunodepleted or mock-immunodepleted extracts (HSS and NPE) were analyzed by immunoblotting against xStn1. The volume of the loaded extracts is 0.2 $\mu$l/lane. Positions of xStn1 protein are indicated. Although the anti-xStn1 antibody detected a single band in immunoblotting experiments using the cell lysates of Sf9 expressing recombinant xStn1, it produced many nonspecific bands in the immunoblotting using the egg extracts. This is probably because the concentration of endogenous xStn1 is so low (5 nM at most, see supplemental Fig. S8) that cross-reactions with proteins other than xStn1 are dominantly detected over the specific interaction between the antibody and xStn1. Unlike xStn1, most of the nonspecific bands detected in the immunoblotting experiments with anti-xStn1 antibody were not immunoprecipitated by anti-xStn1 antibody, suggesting that the antibody immunodepletes proteins with high specificity compared with the immunoblotting experiments (supplemental Fig. S3). Moreover, similar results were obtained when we immunodepleted xStn1 from HSS with two independently immunized anti-xStn1 antibodies that recognized different sets of nonspecific bands (KU003 and KU004, see supplemental Fig. S3), supporting the notion that the biological effects of the immunodepletion observed in *B* are caused by the depletion of xStn1 or its binding proteins. *B, upper*, DNA replication assay using pBluescript dsDNA as template. pBluescript was incubated in xStn1-immunodepleted or mock-immunodepleted HSS for 30 min. Then, 2 volumes of xStn1-immunodepleted or mock-immunodepleted NPE containing [$\alpha$-$^{32}$P]dCTP was added, and the reaction was incubated further. Aliquots were withdrawn at the indicated time points, and DNA was isolated and subjected to agarose gel electrophoresis. Nucleotide incorporation was visualized by autoradiography. *Lower*, DNA replication assay using M13 ssDNA as template. M13 was incubated in xStn1-immunodepleted or mock-immunodepleted extracts containing [$\alpha$-$^{32}$P]dCTP for the indicated times. Nucleotide incorporation was analyzed as described above.

M13 mp18 circular ssDNA (hereafter called M13 for simplicity) is readily converted into dsDNA in *Xenopus* egg extracts in a DNA polymerase $\alpha$-primase-dependent manner (for unknown reasons, NPE does not support M13 replication) (27) (see Fig. 4*B, lower, lanes 10–18*) (28, 29). We found that the efficiency of M13 replication in HSS was significantly decreased in xStn1-immunodepleted HSS compared with mock-immunodepleted HSS (Fig. 4*B, lower, lanes 7–9*). Two independently prepared anti-xStn1 antibodies produced the same results (see Fig. 6, *lanes 1* and *2*), strongly suggesting that the failure of M13 replication was not nonspecific effects of the antibodies, but

was caused by the removal of xStn1 and/or its associated molecules.

Unexpectedly, the addition of recombinant xCST to the xStn1-immunodepleted HSS did not rescue the defect of M13 replication. To explore the possibility that recombinant xCST is not fully functional, we prepared new recombinant xCST (we call it xCST(n) hereafter) that is differently tagged from the original one; untagged xCtc1, untagged xStn1, and C-terminally His$_8$-tagged xTen1. xCST(n) formed a trimeric complex and showed moderate preference for the G-rich sequence as the original one did (supplemental Fig. S6). However, the result of the rescue experiment using xCST(n) was again negative. Although it is possible that both of our recombinant xCSTs are not fully functional, we think that this is unlikely because the addition of xCST(n) to nondepleted HSS enhanced M13 replication (Fig. 5*A*). Furthermore, the neutralizing effect of anti-xStn1 antibody was canceled by xCST(n) (Fig. 5*B*). One possible explanation for the seemingly contradictory data is as follows: xCST-associated molecules cooperate with xCST to support M13 replication, and those molecules are co-immunodepleted by anti-xStn1 antibody. Therefore, the addition of only xCST did not work. The stimulatory effects of adding xCST(n) were observed in Fig. 5 because the co-factors are present in the nondepleted HSS. Taken together, it is unlikely that xCST is irrelevant to M13 replication.

*Priming Is Disturbed in xStn1-depleted Extracts*—M13 replication can be considered as a two-step reaction: initial primer synthesis on a template DNA and subsequent primer extension. To distinguish which of the steps is affected in xStn1-immunodepleted extracts, a short oligo-DNA was annealed to M13, and its replication was assayed in xStn1-immunodepleted HSS (we provide basic data in supplemental Fig. S7 to ensure that the primer is correctly annealed and the replication is initiated from the annealed primer). As shown in Fig. 6, primed M13 was efficiently replicated in both xStn1-immunodeleted and mock-immunodepleted HSSs, whereas nonprimed M13 was poorly replicated in xStn1-immunodepleted HSS.

This result indicates that xStn1-immunodepleted extracts retain the primer extension activity. We conclude that xStn1 and/or its associated factors are involved in the priming of the M13 replication reaction.

*xCST Does Not Affect DNA Polymerase $\alpha$-Primase Binding to Chromatin*—The reduction of the priming activity in xStn1-immunodepleted extracts could be attributed to the inefficient loading of DNA polymerase $\alpha$-primase on M13 in the absence of xStn1. M13 was incubated in xStn1-immunodepleted or mock-immunodepleted HSS, and the reaction mixture was subjected to gel filtration to separate M13 DNA-bound proteins from soluble free proteins. As shown in Fig. 7*A*, M13 DNA was recovered in fractions 12–14 in both cases of mock-immunodepleted and xStn1-immunodepleted extracts. Those fractions were immunoblotted using the antibodies against xStn1, DNA polymerase $\alpha$-primase, or RPA (Fig. 7*B*). DNA polymerase $\alpha$-primase, and RPA were detected similarly in the fractions derived from xStn1-immunodepleted and mock-immunodepleted HSSs containing M13 (Fig. 7*B, lanes 1–6*), but not in the corresponding fractions derived from HSS without M13 (Fig. 7*B, lanes 7–9*). Note that in this experiment, HSS was supple-
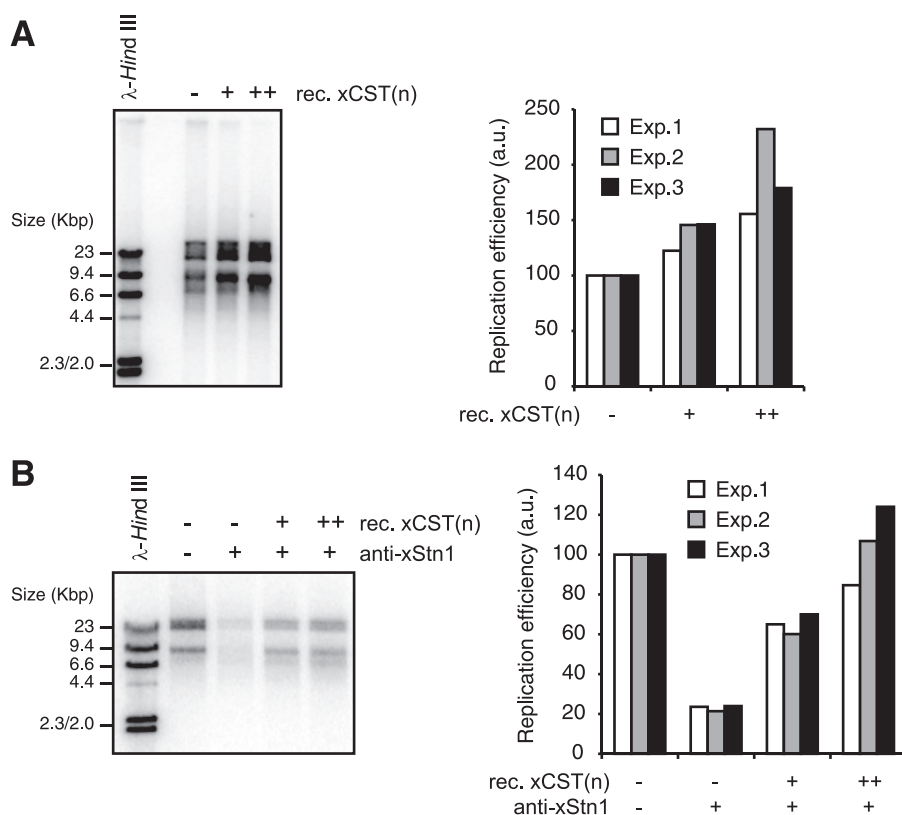
**A**



**B**



FIGURE 5. **xCST(n) enhances M13 replication and reverses the neutralizing effect of anti-xStn1 antibody.** *A*, M13 was incubated in HSS containing [$\alpha$-$^{32}$P]dCTP for 1.5 h in the presence of 0, 0.05, or 0.1 pmol/$\mu$l xCST(n). Replication efficiency, which was determined by measuring radioactivity on the gel, was normalized to the standard condition (without xCST(n) addition). The results of three independent experiments are shown in the *bar graph*. *B*, same experiment as *A*, except that anti-xStn1 KU004 was included in the reactions at the concentration of 0.04 $\mu$g/$\mu$l. The results of three independent experiments are shown in the *bar graph*. Replication efficiency was normalized to the standard condition (without xCST(n) and antibody addition).
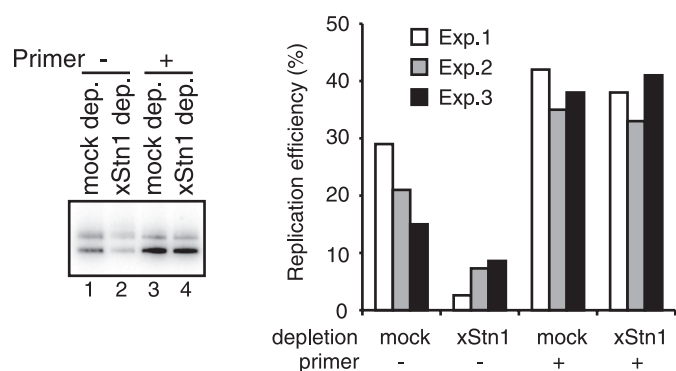


FIGURE 6. **Priming is disturbed in the absence of xStn1.** *Left*, primed or nonprimed M13 was incubated for 1 h in xStn1-immunodepleted or mock-immunodepleted HSS containing [$\alpha$-$^{32}$P]dCTP. KU003 antibody was used to immunodeplete xStn1 (see "Experimental Procedures"). *Right*, radioactivity on the gel was quantified to calculate the amount of newly synthesized DNA in the reactions. Replication efficiency was defined as the ratio of the amount of synthesized DNA to that of input DNA and expressed as percentage. The *graph* shows the results of three independent experiments.

**A**



**B**



FIGURE 7. **xStn1 immunodepletion does not affect DNA polymerase $\alpha$-primase binding to ssDNA in *Xenopus* egg extracts.** *A*, M13 was incubated for 1 h in xStn1-immunodepleted or mock-immunodepleted HSS supplemented with 0.2 mM aphidicolin. The reactions were terminated by transferring the test tubes onto ice, and samples were immediately fractionated by gel filtration. Fractions were collected, and the presence of DNA was revealed by agarose gel electrophoresis followed by SYBR Gold staining. Identities of the circular/linearized forms were determined on the basis of the results shown in supplemental Figs. S4*B* and S7*A*. *B*, fractions 12–14 in *A* were analyzed by immunoblotting using the indicated antibodies. HSS that did not contain M13 DNA was also processed as described in *A* and used for the immunoblotting experiments (*lanes 7-9*). As a reference, 0.2 $\mu$l of HSS was loaded in *lane 10*.

mented with aphidicolin to block DNA synthesis and keep the lengths of single-stranded regions of the template DNA the same between mock-immunodepleted and xStn1-immunodepleted HSSs. Taken together, it was demonstrated that xStn1 and/or its associated proteins are not required for recruiting DNA polymerase $\alpha$-primase to chromatin, but are required for the priming on M13. Our semiquantitative immunoblotting experiments revealed that xStn1 concentration in HSS was at most 5 nM, whereas xRPA concentration was at least 300 nM
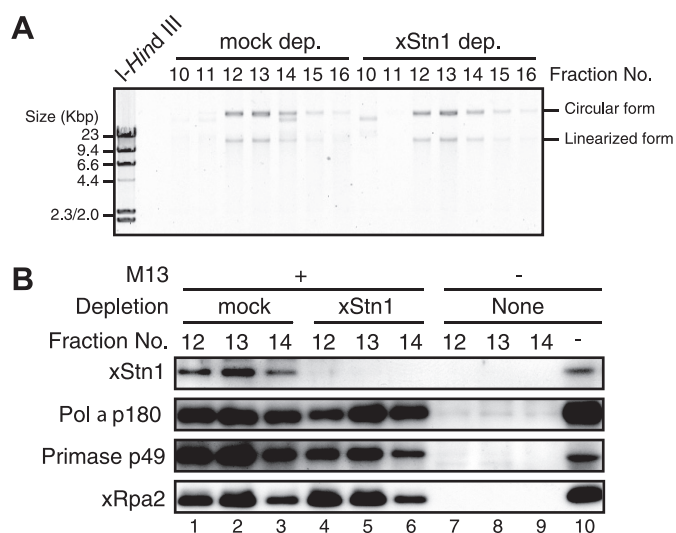
([supplemental Fig. S8](#)). In the M13 replication assays described here, the molar ratio of M13 template DNA to xStn1 was ∼1, suggesting that a considerably small number of xStn1 were available for a single molecule of template DNA.

## DISCUSSION

In this study, *X. laevis* Ctc1, Stn1, and Ten1 genes that encode OB-fold-containing proteins have been identified. They formed a trimeric protein complex that bound to ssDNA with moderate preference for G-rich sequences. xStn1 associated with chromatin independently of DNA replication, and at least a fraction of xStn1 was found to localize at telomeres. *In vitro* DNA replication assays using *Xenopus* egg extracts showed that xCST is not an absolute requirement for the pre-RC-dependent duplex DNA replication, but it and/or its associated factors regulate the priming on ssDNA template. These findings suggest that xCST is involved in the priming that is not directly coupled with fork progression in the canonical DNA replication. C-strand synthesis that compensates for the G-strand extension caused by telomerase and/or the C-strand resection could be an example of such situations. This study also demonstrated the advantage of using *Xenopus* egg extracts in which complex cellular events, such as DNA replication, are recapitulated manageably.

*xCST Compared with RPA*—The structural similarity between Stn1-Ten1 and RPA32-RPA14 (the middle and small subunits of the RPA complex) revealed in budding yeast has led us to conclude that CST is an RPA-like complex (30). Lacking structural information on vertebrate CST to date, however, we do not exactly know to what extent vertebrate CST is similar to RPA. Nevertheless, it should be emphasized that differences, rather than similarities, are of great interest to understand the functions of CST in cells.

In contrast to xRPA that bound to all the tested probes (with the highest affinity toward oligo(dT)), purified recombinant xCST showed moderate preference for G-rich sequences in EMSA, in agreement with previous studies that showed the specific binding to telomeric-G-strand probes for scStn1p, scTen1p, and hSTN1/OBFC1/AAF-44 (31, 32). The cytological evidence also indicates that xStn1 can localize at telomeres, as has been reported in other organisms (5, 6, 30, 32–34). These results suggest the conserved functions of the CST complex at telomeres.

Nevertheless, we still cannot exclude the possibility that xCST plays a role in nontelomeric regions. In fact, M13 DNA does not contain telomeric repeat sequences, whereas its replication is dependent on the presence of xStn1. This implies that xCST can potentially function in any G-rich regions in the genomes. Consistent with this notion, a number of xStn1 foci were observed outside telomeres, which is similar to mammalian CST (5).

One crucial question is how CST is targeted to the regions where it functions. The G-preference of xCST is unlikely to be the sole mechanism that specifies its binding sites because RPA is present in great excess compared with xCST in the egg extracts and capable of binding to G-rich sequences. Post-translational modifications on xCST and/or interactions with unidentified proteins could influence the determination of the

regions where xCST functions, although we have not obtained any direct evidence to support this idea. It would be interesting to ask whether or not CST forms a metastable complex with DNA polymerase α-primase and ssDNA, or whether or not CST favors substrates yet to be examined, such as primer/template junction structures or the G-quartet.

*General Replication Factor or Not?*—Excellent *in vitro* studies have demonstrated the stimulatory effects of mouse CST on DNA polymerase α-primase and essentially, three mechanisms have been proposed: (i) it prevents the enzyme from being released from the replicating template; (ii) it increases the processivity of DNA polymerase α; and (iii) it stimulates primase activity (17, 35, 36).

Casteel *et al.* reported that STN1 (AAF-44) co-localized with proliferating cell nuclear antigen, a marker of replication foci, and *STN1* (*AAF-44*) knockdown by siRNA resulted in the decrease in thymidine uptake in mammalian cell lines (17). These results suggest the roles of CST in general DNA replication. However, we showed previously that hSTN1 did not co-localize with replication foci labeled by the incorporation of a thymidine analog, EdU (5-ethynyl-2′-deoxyuridine). Furthermore, *STN1* knockdown did not cause any defects in cell cycle progression and cell viability.

Here, we showed that xStn1 binding to chromatin was replication-independent and almost kept constant during the interphase of the cell cycle, in stark contrast to the dynamic binding pattern exhibited by typical replication-related factors. Moreover, *Xenopus* cell-free DNA replication systems provided direct evidence that xCST is not required for the pre-RC-dependent replication of dsDNA, and the results led us to the conclusion that xCST is not a general replication factor.

Instead, we found that M13 replication was affected in the absence of xStn1. Because primed M13 replicated in the absence of xStn1, primer extension by DNA polymerases (note that polymerases engaged in the primed M13 replication could be polymerases other than DNA polymerase α) does not necessarily require xStn1. This suggests that the above mentioned mechanisms (i) and (ii), which describe the regulation of DNA polymerase α by CST, are not significant in our system. Because the binding of DNA polymerase α-primase was unaffected in the absence of xStn1, xCST is not a recruiter of DNA polymerase α-primase, either. The most likely interpretation at this time is that the priming is disturbed in the absence of xStn1. Although mechanism (iii) could explain this interpretation, it does not explain why M13 replication is inhibited in NPE that contains xCST and a high concentration of DNA polymerase α-primase. With regard to priming, it is interesting to know that RNA primers are quickly degraded or dissociated from the templates in *Xenopus* egg extracts (27).

To explain our data fully, the prevailing model that CST directly regulates DNA synthesis through the modulation of the activities of polymerizing enzymes may not be sufficient. Another possibility is that xCST also indirectly regulates DNA synthesis, for example, by protecting primers from being attacked by nucleases and/or helicases.

The current attractive hypothesis is that CST regulates telomeric C-strand synthesis by DNA polymerase α-primase, which is coupled with telomerase-dependent G-strand exten-

sion and/or compensatory for C-strand resection (16). Recent studies have demonstrated that the lengths of the telomeric 3′-overhangs increase upon *STN1* knockdown in mammalian cells, which may be interpreted as a defect in C-strand fill-in by DNA polymerase α-primase (5, 37). It should be noted that C-strand synthesis at the very end of telomeres can be considered as a pre-RC-independent DNA replication and thus may be modeled by M13 replication. Because physical interactions between CST and DNA polymerase α-primase in species other than budding yeast have not been observed (including *Xenopus*),[6] we still have few clues to uncover the molecular mechanism of how CST stimulates DNA polymerase α-primase. Further studies are required to understand the molecular details in the interplay between CST and DNA polymerase α-primase.

## REFERENCES

1. Richard, D. J., Bolderson, E., and Khanna, K. K. (2009) *Crit. Rev. Biochem. Mol. Biol.* **44,** 98–116
2. Flynn, R. L., and Zou, L. (2010) *Crit. Rev. Biochem. Mol. Biol.* **45,** 266–275
3. Grandin, N., Reed, S. I., and Charbonneau, M. (1997) *Genes Dev.* **11,** 512–527
4. Grandin, N., Damon, C., and Charbonneau, M. (2001) *EMBO J.* **20,** 1173–1183
5. Miyake, Y., Nakamura, M., Nabetani, A., Shimamura, S., Tamura, M., Yonehara, S., Saito, M., and Ishikawa, F. (2009) *Mol. Cell* **36,** 193–206
6. Surovtseva, Y. V., Churikov, D., Boltz, K. A., Song, X., Lamb, J. C., Warrington, R., Leehy, K., Heacock, M., Price, C. M., and Shippen, D. E. (2009) *Mol. Cell* **36,** 207–218
7. Giraud-Panis, M. J., Teixeira, M. T., Géli, V., and Gilson, E. (2010) *Mol. Cell* **39,** 665–676
8. Price, C. M., Boltz, K. A., Chaiken, M. F., Stewart, J. A., Beilstein, M. A., and Shippen, D. E. (2010) *Cell Cycle* **9,** 3157–3165
9. Schramke, V., Luciano, P., Brevet, V., Guillot, S., Corda, Y., Longhese, M. P., Gilson, E., and Géli, V. (2004) *Nat. Genet.* **36,** 46–54
10. Verdun, R. E., and Karlseder, J. (2006) *Cell* **127,** 709–720
11. Moser, B. A., Subramanian, L., Chang, Y. T., Noguchi, C., Noguchi, E., and Nakamura, T. M. (2009) *EMBO J.* **28,** 810–820
12. Ueno, M. (2010) *Biosci. Biotechnol. Biochem.* **74,** 1–6
13. Gong, Y., and de Lange, T. (2010) *Mol. Cell* **40,** 377–387
14. Baumann, P., and Price, C. (2010) *FEBS Lett.* **584,** 3779–3784
15. Verdun, R. E., Crabbe, L., Haggblom, C., and Karlseder, J. (2005) *Mol. Cell* **20,** 551–561
16. Grossi, S., Puglisi, A., Dmitriev, P. V., Lopes, M., and Shore, D. (2004) *Genes Dev.* **18,** 992–1006
17. Casteel, D. E., Zhuang, S., Zeng, Y., Perrino, F. W., Boss, G. R., Goulian, M., and Pilz, R. B. (2009) *J. Biol. Chem.* **284,** 5807–5818
18. Arias, E. E., and Walter, J. C. (2004) *Front. Biosci.* **9,** 3029–3045
19. Walter, J., Sun, L., and Newport, J. (1998) *Mol. Cell* **1,** 519–529
20. Nabetani, A., Yokoyama, O., and Ishikawa, F. (2004) *J. Biol. Chem.* **279,** 25849–25857
21. Blow, J. J., and Laskey, R. A. (1986) *Cell* **47,** 577–587
22. Murzin, A. G. (1993) *EMBO J.* **12,** 861–867
23. Wold, M. S. (1997) *Annu. Rev. Biochem.* **66,** 61–92
24. Meyne, J., Ratliff, R. L., and Moyzis, R. K. (1989) *Proc. Natl. Acad. Sci. U.S.A.* **86,** 7049–7053
25. Walter, J., and Newport, J. (2000) *Mol. Cell* **5,** 617–627
26. Byun, T. S., Pacek, M., Yee, M. C., Walter, J. C., and Cimprich, K. A. (2005) *Genes Dev.* **19,** 1040–1052
27. MacDougall, C. A., Byun, T. S., Van, C., Yee, M. C., and Cimprich, K. A. (2007) *Genes Dev.* **21,** 898–903
28. Méchali, M., and Harland, R. M. (1982) *Cell* **30,** 93–101
29. Riedel, H. D., König, H., Stahl, H., and Knippers, R. (1982) *Nucleic Acids Res.* **10,** 5621–5635
30. Sun, J., Yu, E. Y., Yang, Y., Confer, L. A., Sun, S. H., Wan, K., Lue, N. F., and Lei, M. (2009) *Genes Dev.* **23,** 2900–2914
31. Gao, H., Cervantes, R. B., Mandell, E. K., Otero, J. H., and Lundblad, V. (2007) *Nat. Struct. Mol. Biol.* **14,** 208–214
32. Wan, M., Qin, J., Songyang, Z., and Liu, D. (2009) *J. Biol. Chem.* **284,** 26725–26731
33. Martín, V., Du, L. L., Rozenzhak, S., and Russell, P. (2007) *Proc. Natl. Acad. Sci. U.S.A.* **104,** 14038–14043
34. Li, S., Makovets, S., Matsuguchi, T., Blethrow, J. D., Shokat, K. M., and Blackburn, E. H. (2009) *Cell* **136,** 50–61
35. Goulian, M., Heard, C. J., and Grimm, S. L. (1990) *J. Biol. Chem.* **265,** 13221–13230
36. Goulian, M., and Heard, C. J. (1990) *J. Biol. Chem.* **265,** 13231–13239
37. Dai, X., Huang, C., Bhusari, A., Sampathi, S., Schubert, K., and Chai, W. (2010) *EMBO J.* **29,** 2788–2801